

Modeling Multivariate Positive-Valued Time Series Using R-INLA

Chiranjit Dutta ^{*a}, Nalini Ravishanker^b, and Sumanta Basu^c

^{a,b}Department of Statistics, University of Connecticut, Storrs, CT, USA

^cDepartment of Statistics and Data Science, Cornell University, Ithaca, NY, USA

July 5, 2022

Abstract

In this paper we describe fast Bayesian statistical analysis of vector positive-valued time series, with application to interesting financial data streams. We discuss a flexible level correlated model (LCM) framework for building hierarchical models for vector positive-valued time series. The LCM allows us to combine marginal gamma distributions for the positive-valued component responses, while accounting for association among the components at a latent level. We use integrated nested Laplace approximation (INLA) for fast approximate Bayesian modeling via the `R-INLA` package, building custom functions to handle this setup. We use the proposed method to model interdependencies between realized volatility measures from several stock indexes.

Keywords: Positive time series, Level correlated models, Multivariate gamma, Approximate Bayesian inference, INLA, Realized volatility

1 Introduction

Multivariate positive-valued time series are ubiquitous across diverse application domains, including but not limited to, epidemiology, econometrics, finance, insurance, and signal processing. In financial applications, we increasingly observe long multivariate positive-valued time series from multiple stocks. Examples include time series related to high-frequency trading, such as volume, price, realized volatility measures, durations, etc. While there has been a considerable amount of research on modeling univariate positive-valued time series with exponential and gamma marginals (Lawrance and Lewis (1980, 1981, 1985), Jacobs and Lewis (1977), Raftery (1982), Gaver and Lewis (1980) and Gouriéroux and Jasiak (2006)), research on the multivariate setup is rather limited. A few references which deal with modeling multivariate positive-valued time series include Prékopa and Szántai (1978), Yue (2001), Cipollini et al. (2006) and Hautsch et al. (2013). While these *static* modeling approaches may be useful when the time series are stationary, many interesting situations in practice involve nonstationary time series and will benefit from fitting *dynamic* models.

Gaussian dynamic models have been widely used for several decades for modeling univariate and multivariate time series (West and Harrison, 2006, Petris, 2010). More recently, dynamic generalized linear models (DGLM's) have been tailored to model non-Gaussian time series without the necessity of data transformations, or other adaptations; see West et al. (1985), Grunwald et al. (1993), Fahrmeir and Kaufmann (1987), Lindsey and Lambert (1995), Gamerman (1998), Chiogna et al. (2002), Shephard and Pitt (1997), Benjamin et al. (2003) and Godolphin and Triantafyllopoulos (2006). Fahrmeir et al. (1994) and Durbin and Koopman (2012) are excellent books on this topic.

Non-Gaussian dynamic modeling with marginals having positive support (such as gamma, lognormal, or Weibull) is an attractive setup for analyzing multivariate positive-valued series exhibiting temporal non-stationarity, as well as skewness and heavy-tails. Univariate gamma regression models for each of the components of the response vector cannot account for the dependence among the components, where the

*Corresponding Author: chiranjit.dutta@uconn.edu

dependence may be due to omitted variables which simultaneously effect the response vector (Aitchison and Ho, 1989, Chib and Winkelmann, 2001, Ma et al., 2008). Therefore, an adequate multivariate model for positive time series is needed.

To our knowledge, Aktekin et al. (2020) is the only paper describing a dynamic model for multivariate positive-valued time series. It accounts for correlations among the components through a common random environment that evolves over time. They develop MCMC methods as well as sequential Monte Carlo methods for parameter estimation. Tsionas (2004) described Bayesian analysis using a multivariate gamma likelihood (Mathai and Moschopoulos, 1991), non-conjugate prior specifications, and Gibbs sampler with data augmentation. This is not a dynamic model, and moreover, computing the likelihood function can be cumbersome and time consuming. Incorporating the dependence among the components of the positive-valued vector through a different mechanism will be useful. In general, using Markov chain Monte Carlo (MCMC) methods for Bayesian hierarchical dynamic modeling of vector positive-valued time series under a multivariate gamma sampling distributional assumption may be computationally demanding, especially since there does not exist any convenient form of the likelihood function.

The level correlated model (LCM) framework described in Serhiyenko (2015) for multivariate time series of counts offers a computationally simpler way of handling dependency among the components in vector-valued responses. We adapt this framework for modeling multivariate positive-valued time series, which assumes marginal gamma component distributions, and accounts for the association between the components at a latent Gaussian level. This avoids the need for computing the multivariate gamma likelihood, which can be computationally demanding.

Another way to reduce the computational burden is to replace the MCMC approach by the integrated nested Laplace approximation (INLA) approach. INLA enables approximate Bayesian inference for a large class of latent Gaussian models (LGMs) with wide-ranging applications Rue et al. (2009), and unlike simulation intensive Bayesian approaches, it performs approximate inference using a series of deterministic approximations that take advantage of the LGM structure to provide fast and accurate inference. Ruiz-Cárdenas et al. (2012) presented a general framework which enabled users to use R-INLA for a variety of state-space models. Serhiyenko et al. (2015, 2018) used multivariate Gaussian random effects to model level correlated effect in multivariate time series of counts in the LCM framework thus facilitating the estimation of LCMs using R-INLA package.

In this article, we describe the LCM framework for dynamic modeling of vector positive-valued time series. At the observation level, the components are conditionally independent with marginal gamma distributions, while a level correlation random effect knits the dependence between components. The latent state vector evolves as a stationary vector autoregression (VAR) or vector autoregression and moving average (VARMA) process. We use R-INLA for the data analysis, developing custom code via the `rgeneric()` function for implementing the VAR or VARMA latent models. This setup is useful for financial modeling of the joint dynamics of realized volatility measures among the stock indexes.

The format of the paper follows. Section 2 describes the general framework of the level correlated model (LCM). Section 3 gives the description of the approximate Bayesian analysis using R-INLA including the derivation of the joint distribution of the latent states in subsection 3.1, followed by the prior specification and model fitting using R-INLA in subsection 3.2. For simulated data, Section 4 demonstrates that the R-INLA approach enables accurate model fitting. Section 5 presents an analysis of the multivariate realized measures of volatility. Finally, Section 6 concludes with discussion and directions for future research.

2 Level Correlated Model Framework

Let $\mathbf{y}_{it} = (Y_{1,it}, \dots, Y_{m,it})'$ be a m -variate vector of continuous positive responses for $i = 1, \dots, n$ and $t = 1, \dots, T$. In the financial example, we would observe m components of positive responses on n stocks over T days. We describe the LCM setup for positive responses similar to the description in Serhiyenko (2015). In the following, we let $i = 1 \dots n$, $t = 1 \dots T$, and $j = 1 \dots m$. Assuming gamma marginals for the components, the observation equation can be written as

$$Y_{j,it} | \theta_{j,it}, \tau \sim \text{Gamma} \left(\tau, \frac{\tau}{\theta_{j,it}} \right), \quad (1)$$

where the precision parameter $\tau > 0$ is static, and the random mean $\theta_{j,it} > 0$. Then, $E(Y_{j,it}|\theta_{j,it}, \tau) = \theta_{j,it}$, and $\text{Var}(Y_{j,it}|\theta_{j,it}, \tau) = \theta_{j,it}^2/\tau$. A dynamic model for the random mean $\theta_{j,it}$ is

$$\log(\theta_{j,it}) = \beta_{j,i0} + x_{j,t} + \mathbf{S}'_{j,it}\boldsymbol{\beta}_{j,i} + \alpha_{j,it}, \quad (2)$$

where the random effect $\beta_{j,i0}$ is a subject-specific intercept corresponding to the j th component of the response, $x_{j,t}$ is a time-varying latent state vector which depends on the j th component, and the random effect $\alpha_{j,it}$ is a response type, time, and subject-specific level correlated error component. The vector $\mathbf{S}'_{j,it}$ denotes a p_j -dimensional vector of covariates, and $\boldsymbol{\beta}_{j,i}$ is a corresponding p_j -dimensional vector of coefficients. In general, $\boldsymbol{\beta}_{j,i}$ can also be treated as time-varying. We have chosen to use the logarithmic link function in (2) corresponding to the gamma marginals in (1), but other suitable link functions may also be used. Let the level correlation vector $\boldsymbol{\alpha}_{it} = (\alpha_{1,it}, \dots, \alpha_{m,it})'$. The dependence between the components of \mathbf{y}_{it} can be introduced via $\boldsymbol{\alpha}_{it} \sim N(\mathbf{0}, \boldsymbol{\Sigma})$, where $\boldsymbol{\Sigma}$ is a variance-covariance matrix for the level correlated error. More generally, we can allow $\boldsymbol{\Sigma}$ to be a subject-specific parameter and assume that $\boldsymbol{\alpha}_{it} \sim N(\mathbf{0}, \boldsymbol{\Sigma}_i)$.

We specify the evolution of the latent state vector $\mathbf{x}_t = (x_{1,t}, \dots, x_{m,t})'$ via a vector autoregression, VAR(p), given by

$$\mathbf{x}_t = \sum_{h=1}^p \boldsymbol{\Phi}_h \mathbf{x}_{t-h} + \mathbf{w}_t = \boldsymbol{\Phi}(B)\mathbf{x}_t + \mathbf{w}_t, \quad (3)$$

where $t = 1 \dots T$, $\boldsymbol{\Phi}_h$ are coefficient matrices of order $m \times m$ and the error vector $\mathbf{w}_t \sim N(\mathbf{0}, \mathbf{W})$, \mathbf{W} being a $m \times m$ state error variance-covariance matrix. In (3), $\boldsymbol{\Phi}(B)$ is the VAR(p) operator defined as

$$\boldsymbol{\Phi}(B) = \mathbf{I}_m - \boldsymbol{\Phi}_1 B - \dots - \boldsymbol{\Phi}_p B^p, \quad (4)$$

where B is the back-shift operator such that $B^j \mathbf{x}_t = \mathbf{x}_{t-j}$, for any $j \geq 1$. The VAR(p) process is stationary if the roots of the determinant of $\boldsymbol{\Phi}(z)$ are outside the unit circle, i.e., the modulus of each root is greater than 1, (Lütkepohl, 2005). We refer to the model defined by (1)-(3) as an LCM-VAR, with independent gamma marginals at the observation level. Let $\boldsymbol{\Theta}^* = (\beta_{j,i0}, \boldsymbol{\beta}'_{j,i}, \text{vec}'(\boldsymbol{\Sigma}), \text{vec}'(\boldsymbol{\Phi}_1), \dots, \text{vec}'(\boldsymbol{\Phi}_p), \text{vec}'(\mathbf{W}))'$ denote the set of all LCM-VAR parameters, where vec is the vectorization operator.

If the $\boldsymbol{\Phi}_h$ matrices in (3) are all assumed to be diagonal, the LCM-VAR model simplifies to m separate LCM-AR models, again with independent gamma marginals. Here, each component of the latent state vector \mathbf{x}_t evolves according to an autoregressive (AR) process of order p , and the state equation (3) becomes

$$x_{j,t} = \sum_{h=1}^p \phi_{j,h} x_{j,(t-h)} + w_{j,t}, \quad j = 1, \dots, m, \quad (5)$$

where the error $w_{j,t} \sim N(0, W_j)$, for scalar W_j .

3 Approximate Bayesian Analysis using INLA

In the LCM framework, it is possible to use R-INLA templates when the state equation follows (5), but not when it follows the VAR(p) model in (3). To implement a model with latent VAR effects, we can use the `rgeneric()` function to code the joint p.d.f. of the state vector \mathbf{x}_t which is described in the next section.

3.1 Joint Distribution of the Latent States

Suppose $\mathbf{x}_t = (X_{t,1}, \dots, X_{t,m})'$ is an m -dimensional latent process in (3). Let $\boldsymbol{\Theta}$ denote the vector of all the parameters. The latent Gaussian Markov field representation is that of a multivariate Gaussian vector with a sparse precision matrix as in (Rue and Held, 2005, Palmí-Perales et al., 2021); i.e.,

$$\text{vec}(\boldsymbol{\Theta}) \sim N(\mathbf{0}, \boldsymbol{\Sigma}^*), \quad (6)$$

where $\mathbf{0}$ denotes vector of zeros and $\boldsymbol{\Sigma}^*$ is the variance-covariance matrix. Since R-INLA works with the precision matrix, we derive the form of the joint p.d.f. in terms of $\boldsymbol{\Sigma}^{*-1}$. We first show the form of the joint p.d.f. for the VAR(1) latent process.

3.1.1 Joint p.d.f. for a VAR(1) Process

When $p = 1$, (3) simplifies to a VAR(1) process:

$$\mathbf{x}_t = \Phi \mathbf{x}_{t-1} + \mathbf{w}_t. \quad (7)$$

To derive the joint distribution of $(\mathbf{x}'_1, \dots, \mathbf{x}'_T)'$, we see that

$$\log \pi(\mathbf{x}_t | \mathbf{x}_{t-1}) = -\frac{1}{2} \mathbf{w}'_t \mathbf{W}^{-1} \mathbf{w}_t + C,$$

where $\mathbf{w}_t = \mathbf{x}_t - \Phi \mathbf{x}_{t-1}$, $\pi(\cdot)$ denotes the probability density function and C is a constant. We assume diffuse initial conditions for $\mathbf{x}_1 \sim N(\mathbf{0}, \frac{1}{\kappa} \mathbf{I}_m)$, where $\kappa = 0.01$. The joint distribution of $(\mathbf{x}'_1, \dots, \mathbf{x}'_T)'$ is given by

$$\begin{aligned} \log \pi(\mathbf{x}_1, \mathbf{x}_2, \dots, \mathbf{x}_n) &= \sum_{t=2}^n \log \pi(\mathbf{x}_t | \mathbf{x}_{t-1}) + \log \pi(\mathbf{x}_1) \\ &= -\frac{1}{2} [(\mathbf{x}_n - \Phi \mathbf{x}_{n-1})' \mathbf{W}^{-1} (\mathbf{x}_n - \Phi \mathbf{x}_{n-1}) + (\mathbf{x}_{n-1} - \Phi \mathbf{x}_{n-2})' \mathbf{W}^{-1} (\mathbf{x}_{n-1} - \Phi \mathbf{x}_{n-2}) \\ &\quad + \dots + (\mathbf{x}_2 - \Phi \mathbf{x}_1)' \mathbf{W}^{-1} (\mathbf{x}_2 - \Phi \mathbf{x}_1) + \mathbf{x}'_1 \kappa \mathbf{I}_m \mathbf{x}_1] + C' \\ &= -\frac{1}{2} [\mathbf{x}'_n \mathbf{W}^{-1} \mathbf{x}_n - \mathbf{x}'_n \mathbf{W}^{-1} \Phi \mathbf{x}_{n-1} - \mathbf{x}'_{n-1} \Phi' \mathbf{W}^{-1} \mathbf{x}_n + \mathbf{x}'_{n-1} (\Phi' \mathbf{W}^{-1} + \mathbf{W}^{-1}) \mathbf{x}_{n-1} \\ &\quad + \dots + \mathbf{x}'_2 (\Phi' \mathbf{W}^{-1} \Phi \mathbf{x}_2 + \mathbf{W}^{-1}) \mathbf{x}_2 - \mathbf{x}'_2 \mathbf{W}^{-1} \Phi' \mathbf{x}_1 - \mathbf{x}'_1 \Phi' \mathbf{W}^{-1} \mathbf{x}_2 \\ &\quad + \mathbf{x}'_1 (\Phi' \mathbf{W}^{-1} \Phi + \kappa \mathbf{I}_m) \mathbf{x}_1] + C' \end{aligned}$$

Let $\mathbf{A} = \Phi' \mathbf{W}^{-1} \Phi$, $\mathbf{B} = -\Phi' \mathbf{W}^{-1}$ and $\mathbf{C} = \mathbf{W}^{-1}$ be the $m \times m$ matrices and let $\mathbf{0}_m$ be the $m \times m$ matrix of 0's. Hence the precision matrix for the joint distribution of $(\mathbf{x}'_1, \dots, \mathbf{x}'_T)'$ is a $mT \times mT$ matrix given by

$$\Sigma^{*-1} = \begin{bmatrix} \mathbf{A} + \kappa \mathbf{I}_m & \mathbf{B} & \dots & \dots & \dots & \dots & \dots & \mathbf{0}_m \\ \mathbf{B}' & \mathbf{A} + \mathbf{C} & \mathbf{B} & \ddots & & & & \vdots \\ \vdots & \mathbf{B}' & \mathbf{A} + \mathbf{C} & \mathbf{B} & & & & \vdots \\ \vdots & \ddots & \ddots & \ddots & \ddots & \ddots & & \vdots \\ \vdots & & \ddots & \ddots & \ddots & \ddots & \ddots & \vdots \\ \vdots & & & \ddots & \ddots & \ddots & \ddots & \mathbf{0}_m \\ \vdots & & & & \ddots & \ddots & \ddots & \mathbf{B} \\ \mathbf{0}_m & \dots & \dots & \dots & \dots & \mathbf{0}_m & \mathbf{B}' & \mathbf{C} \end{bmatrix}, \quad (8)$$

3.1.2 Joint p.d.f. for a VAR(p) Process

Following Lütkepohl (2005), we can represent a VAR(p) process of an m -dimensional time series (in (3)) as a VAR(1) process of a pm -dimensional time series, by stacking $\mathbf{x}_t, \mathbf{x}_{t-1}, \dots, \mathbf{x}_{t-p+1}$:

$$\begin{pmatrix} \mathbf{x}_t \\ \mathbf{x}_{t-1} \\ \mathbf{x}_{t-2} \\ \vdots \\ \vdots \\ \mathbf{x}_{t-p+1} \end{pmatrix} = \begin{pmatrix} \Phi_1 & \Phi_2 & \dots & \dots & \Phi_{p-1} & \Phi_p \\ \mathbf{I}_m & \mathbf{0}_m & \ddots & & \mathbf{0}_m & \mathbf{0}_m \\ \mathbf{0}_m & \mathbf{I}_m & \ddots & \ddots & \mathbf{0}_m & \mathbf{0}_m \\ \vdots & \vdots & \ddots & \ddots & \vdots & \vdots \\ \mathbf{0}_m & \mathbf{0}_m & \dots & \dots & \mathbf{I}_m & \mathbf{0}_m \end{pmatrix} \begin{pmatrix} \mathbf{x}_{t-1} \\ \mathbf{x}_{t-2} \\ \mathbf{x}_{t-3} \\ \vdots \\ \vdots \\ \mathbf{x}_{t-p} \end{pmatrix} + \begin{pmatrix} \mathbf{w}_t \\ \mathbf{0} \\ \mathbf{0} \\ \vdots \\ \vdots \\ \mathbf{0} \end{pmatrix}, \text{ i.e.,} \quad (9)$$

$$\mathbf{x}_t^* = \Phi^* \mathbf{x}_{t-1}^* + \mathbf{w}_t^*,$$

where $\mathbf{w}_t^* \sim SN(\mathbf{0}, \mathbf{W}^*)$, $\mathbf{W}^* = \begin{pmatrix} \mathbf{W} & \mathbf{0}_m & \dots & \mathbf{0}_m \\ \vdots & \vdots & \ddots & \vdots \\ \mathbf{0}_m & \mathbf{0}_m & \dots & \mathbf{0}_m \end{pmatrix}$ is a $pm \times pm$ p.s.d. matrix and SN denotes a singular normal distribution.

Following the setup for the VAR(1) process in Section 3.1.1, we can then obtain the $pmT \times pmT$ dimensional precision matrix for the joint distribution of T realizations from a VAR(p) process as

$$\Sigma^{*-1} = \begin{bmatrix} \mathbf{A}^* + \kappa^* \mathbf{I}_m & \mathbf{B}^* & \cdots & \cdots & \cdots & \cdots & \cdots & \mathbf{0}_m \\ \mathbf{B}^{*'} & \mathbf{A}^* + \mathbf{C}^* & \mathbf{B}^* & \ddots & & & & \vdots \\ \vdots & \mathbf{B}^{*'} & \mathbf{A}^* + \mathbf{C}^* & \mathbf{B}^* & & & & \vdots \\ \vdots & \ddots & \ddots & \ddots & \ddots & \ddots & \ddots & \vdots \\ \vdots & & & \ddots & \ddots & \ddots & \ddots & \vdots \\ \vdots & & & & \ddots & \ddots & \ddots & \mathbf{0}_m \\ \vdots & & & & & \ddots & \ddots & \mathbf{B}^* \\ \mathbf{0}_m & \cdots & \cdots & \cdots & \cdots & \mathbf{0}_m & \mathbf{B}^{*'} & \mathbf{C}^* \end{bmatrix}, \quad (10)$$

where, $\mathbf{A}^* = \Phi^{*'} \mathbf{W}^{*+} \Phi^*$, $\mathbf{B}^* = -\Phi^{*'} \mathbf{W}^{*+}$ and $\mathbf{C}^* = \mathbf{W}^{*+}$ are $pm \times pm$ matrices and \mathbf{W}^{*+} denotes the Moore-Penrose inverse. Let $\Psi = (\text{vec}(\Phi_1)', \dots, \text{vec}(\Phi_p)', \text{vec}(\mathbf{W})')$ be the vector of parameters and let $\mathbf{x} = (\mathbf{x}_1', \dots, \mathbf{x}_T')$ be the observations from a VAR(p) process. The joint p.d.f. is given by

$$f(\mathbf{x}|\Psi) = (2\pi)^{-pmT/2} |\Sigma^*|^{-1/2} \exp\left(-\frac{1}{2} \mathbf{x}' \Sigma^{*-1} \mathbf{x}\right). \quad (11)$$

3.1.3 Joint p.d.f. for a VARMA(p, q) Process

In the literature, we rarely see applications where the state evolution in a dynamic model follows a VARMA process. Nevertheless, for completeness, we derive the precision matrix for the joint p.d.f. of an m -dimensional time series following a stationary VARMA(p, q) process defined by

$$\Phi(B)\mathbf{x}_t = \Theta(B)\mathbf{w}_t, \quad (12)$$

where $\Phi(B)$ is the VAR operator as defined in (4) and the moving average (MA) operator $\Theta(B)$ is defined as

$$\Theta(B) = \mathbf{I}_m - \Theta_1 B - \dots - \Theta_q B^q.$$

In (12), Φ_i and Θ_i are $m \times m$ unknown parameter matrices and the m -dimensional white noise process is represented by $\mathbf{w}_t = (w_{t,1}, \dots, w_{t,m})$ with $E(\mathbf{w}_t) = \mathbf{0}$ and $Cov(\mathbf{w}_t) = \Sigma_w$, which a p.d. variance-covariance matrix. Let $\Psi^* = (\text{vec}(\Phi_1)', \dots, \text{vec}(\Phi_p)', \text{vec}(\Theta_1)', \dots, \text{vec}(\Theta_q)', \text{vec}(\Sigma_w)')$ be the vector of parameters and assuming Gaussian errors, the joint p.d.f. is given by

$$L(\Psi^*|\mathbf{x}) = (2\pi)^{-mT/2} |\Sigma|^{-1/2} \exp\left(-\frac{1}{2} \mathbf{x}' \Sigma^{-1} \mathbf{x}\right), \quad (13)$$

where T is the number of observations, $\mathbf{x} = (\mathbf{x}_1', \dots, \mathbf{x}_T')$ is mT -dimensional vector and Σ is the $mT \times mT$ variance-covariance matrix of the observations. Using the closed form expressions in Gallego (2009), we have

$$L(\Psi^*|\mathbf{x}) = L(\Psi^*|\hat{\mathbf{w}}_0) = (2\pi)^{-mT/2} |\Sigma_0|^{-1/2} \exp\left(-\frac{1}{2} \hat{\mathbf{w}}_0' \Sigma_0^{-1} \hat{\mathbf{w}}_0\right), \quad (14)$$

where Σ_0 is the variance-covariance matrix of $\hat{\mathbf{w}}_0$. Let $\mathbf{u} = (\mathbf{x}_{-p+1}, \dots, \mathbf{x}_0, \mathbf{w}_{-q+1}, \dots, \mathbf{w}_0)$ is a $m(p+q) \times 1$ vector of pre-sample values and covariance of pre-sample values be given by Σ_u . The block matrix $\Phi = [\Phi_{ij}]$ ($i = 1, \dots, T; j = 1, \dots, T$) is defined as $\Phi_{ij} = -\Phi_{i-j}$ for $0 \leq i-j \leq p$ and $\Phi_{ij} = \mathbf{0}$ otherwise, where the $m \times m$ matrix Φ_{ij} is the typical block of Φ and $\Phi_0 = -\mathbf{I}_m$. Similarly, the block matrix $\Theta = [\Theta_{ij}]$ ($i = 1, \dots, T; j = 1, \dots, T$) is such that $\Theta_{ij} = -\Theta_{i-j}$ for $0 \leq i-j \leq q$ and $\Theta_{ij} = \mathbf{0}$ otherwise, where $\Theta_0 = -\mathbf{I}_m$. Let $r = \max(p, q)$ and the block matrix $\mathbf{F} = [\mathbf{F}_{ij}]$ ($i = 1, \dots, r; j = 1, \dots, p+q$) is such that $\mathbf{F}_{ij} = \Phi_{p-(j-i)}$ for $0 \leq j-i < p$, $\mathbf{F}_{ij} = -\Theta_{p+q-(j-i)}$ for $p \leq j-i < p+q$, and $\mathbf{F}_{ij} = \mathbf{0}$ otherwise. The $kT \times kr$ matrix \mathbf{G} has 1s along the main diagonal and 0s otherwise. Hence the precision matrix as in Gallego (2009) is given by

$$\Sigma_0^{-1} = (\mathbf{I}_T \otimes \Sigma_w^{-1}) - (\mathbf{I}_T \otimes \Sigma_w^{-1}) \Theta^{-1} \mathbf{G} \mathbf{F} (\mathbf{Z}' \mathbf{Z})^{-1} \mathbf{F}' \mathbf{G}' \Theta^{-1} (\mathbf{I}_T \otimes \Sigma_w^{-1}), \quad (15)$$

where

$$\mathbf{Z}'\mathbf{Z} = \Sigma_u^{-1} + \mathbf{F}'\mathbf{G}'\Theta^{-1} (\mathbf{I}_T \otimes \Sigma_w^{-1}) \Theta^{-1} \mathbf{G}\mathbf{F}$$

is a square matrix of order $m(p+q)$.

3.2 Approximate Posterior Analysis

Let \mathbf{Y} and \mathbf{S} respectively denote the responses \mathbf{y}_{it} and the static predictors $\mathbf{S}'_{j,it}$ for $i = 1, \dots, n$, $j = 1, \dots, m$ and $t = 1, \dots, T$. Let $\mathbf{b} = (\beta_{ji0}, \beta'_{j,i})'$ denote all the subject-specific intercepts β_{ji0} and the fixed effects $\beta_{j,i}$, for $i = 1, \dots, n$ and $j = 1, \dots, m$, $\Phi = (\text{vec}'(\Phi_1), \dots, \text{vec}'(\Phi_p))'$ denote all the parameters related to the coefficient matrices in the latent states and let $\mathbf{x} = (\mathbf{x}'_1, \dots, \mathbf{x}'_T)'$ denotes the latent states. Let τ be the precision parameter of the observation equation and $\theta_{it} = (\theta_{1,it}, \dots, \theta_{m,it})'$, where $\theta_{j,it}$ evolves as in (2) for $j = 1, \dots, m$. The likelihood function under the model described by equations (1) - (3) is:

$$L(\mathbf{b}, \Phi, \mathbf{W}, \Sigma, \mathbf{x}, \tau | \mathbf{Y}, \mathbf{S}) = \int \prod_{i=1}^n \prod_{t=1}^T p(\mathbf{y}_{it} | \theta_{it}, \tau) \times p(\mathbf{x}_t | \mathbf{x}_{t-1}, \dots, \mathbf{x}_{t-p}, \mathbf{W}) \times p(\alpha_{it} | \Sigma) d\alpha_{it}, \quad (16)$$

where

$$p(\mathbf{y}_{it} | \theta_{it}, \tau) = \prod_{j=1}^m \left(\frac{\tau^\tau}{\Gamma(\tau)\theta_{j,it}^\tau} y_{j,it}^{\tau-1} \exp\left(-\frac{\tau}{\theta_{j,it}} y_{j,it}\right) \right),$$

$$p(\alpha_{it} | \Sigma) = \frac{1}{\sqrt{(2\pi)^m \det(\Sigma)}} \exp\left(-\frac{1}{2}(\alpha'_{it} \Sigma^{-1} \alpha_{it})\right)$$

and $\prod_{t=1}^T p(\mathbf{x}_t | \mathbf{x}_{t-1}, \dots, \mathbf{x}_{t-p}, \mathbf{W})$ is the joint p.d.f. of VAR(p) process and hence can be computed as in (11).

The LCM model parameters include the subject-specific intercepts $\beta_{j,i0}$, the fixed effects $\beta_{j,i}$ - a p_j dimensional vector corresponding to $\mathbf{S}'_{j,it}$, the $m \times m$ variance-covariance matrix of the random effects Σ and the $m \times m$ variance-covariance matrix of the state errors \mathbf{W} . We have mostly used the default prior specifications of R-INLA which seem to work well. A Wishart distribution is considered as a prior specification for the $m \times m$ covariance matrix Σ . In particular, the precision matrix $\Sigma^{-1} \sim \text{Wishart}_m(r, \mathbf{I}_m)$, r is the degree of freedom, whose default value is $2m+1$ representing the default prior specification for m -variate Gaussian random effects in R-INLA. For modeling purposes we have used a diagonal matrix specification for $\mathbf{W} = \text{diag}(\sigma_{w1}^2, \dots, \sigma_{wm}^2)$, where σ_{wj}^2 are marginal variances for $j = 1, \dots, m$. Let the corresponding log-precision be given by $\theta_{wj} = \log\left(\frac{1}{\sigma_{wj}^2}\right)$. Then for each j , the logarithm of the precision θ_{wj} is assumed to follow a log-gamma distribution, whose shape and inverse scale parameters are 1 and 0.00005 respectively. This is also the default prior specification for R-INLA. The prior for the fixed effects is chosen to be the default Gaussian prior with mean 0 and precision 0.001.

Given the data and model parameters, the Bayesian formulation requires specification of the likelihood and prior, from which, using Bayes' Theorem, we obtain the posterior density as a normalized product of the likelihood and prior. Since the likelihood (16) is not available in closed form, its exact analysis is cumbersome. The high computational requirements of a fully Bayesian approach has prompted us to use R-INLA for model fitting (Rue et al., 2009, Lindgren and Rue, 2015). For approximate Bayesian inference, INLA uses nested Laplace approximations and numerical integration, thereby significantly reducing the computational time compared to a fully Bayesian inference via MCMC.

One of the main advantages of INLA is that templates for many useful models in the literature are available in the R-INLA package. Other cases can be programmed and implemented using generic functions. We provide more details about the implementation of VAR(1) as a latent process using `rgeneric` in R-INLA in the Appendix (6). In the following section we show accurate estimation of parameters using simulated data from trivariate LCM-AR and trivariate LCM-VAR and then we fit trivariate LCMs to model interdependencies between the realized volatility measures for several stock indexes.

4 Simulated Data

Data from the trivariate LCM-AR model with $Y_{j,it}$ ($i = 1, \dots, 30$; $j = 1, 2, 3$ and $t = 1, \dots, 500$) is simulated according to the following model:

$$\begin{aligned} Y_{j,it} | \theta_{j,it}, \tau &\sim \text{Gamma}\left(\tau, \frac{\tau}{\theta_{j,it}}\right) \\ \log(\theta_{j,it}) &= x_{j,t} + \alpha_{j,it} + \beta S_{j,it}, \end{aligned} \quad (17)$$

where $S_{j,it}$ represents a static predictor which is simulated from $N(0, 1)$ and $\beta = 0.2$. The state equations are given by (5) with the order of autoregression $p = 1$, $\phi_{1,1} = \phi_{2,1} = \phi_{3,1} = 0.8$ and the state errors $w_{1,t}$, $w_{2,t}$ and $w_{3,t}$ are simulated from $N(0, W_1)$, $N(0, W_2)$ and $N(0, W_3)$ respectively, where $W_1 = 0.3$, $W_2 = 0.2$ and $W_3 = 0.5$. The level correlated term α_{it} is simulated from $N_3(\mathbf{0}, \Sigma)$, where

$$\Sigma = \begin{pmatrix} \sigma_1^2 & \rho_{12}\sigma_1\sigma_2 & \rho_{13}\sigma_1\sigma_3 \\ \rho_{12}\sigma_1\sigma_2 & \sigma_2^2 & \rho_{23}\sigma_2\sigma_3 \\ \rho_{13}\sigma_1\sigma_3 & \rho_{23}\sigma_2\sigma_3 & \sigma_3^2 \end{pmatrix}, \quad (18)$$

is the variance-covariance matrix with $\sigma_1^2 = \sigma_2^2 = \sigma_3^2 = 0.5$ and $\rho_{12} = 0.8$, $\rho_{13} = 0.7$ and $\rho_{23} = 0.5$. The responses are simulated from gamma distribution with $\tau = 300$. For the model estimation, we used the R-INLA package Rue et al. (2009), Martins et al. (2013) with the default prior specification for the parameters as discussed in subsection 3.2. We assume a normal prior for β , trivariate inverse Wishart prior for the variance-covariance matrix Σ and gamma prior for the precisions. We explicitly assumed $\tau \sim \text{Gamma}(0.01, 0.01)$ i.e. $E[\tau] = 1$ and $\text{Var}[\tau] = 100$.

Simulations were conducted on a personal laptop (11th Gen Intel(R) Core(TM) i7-1165G7 @ 2.80GHz) with 16Gb of RAM using 64-bit version of Windows 11 operating system. It took about 7 minutes to run LCM-AR on the simulated data. Most of the estimated parameters in LCM-AR are close to their true values, except for τ , the precision parameter of the observational equation, whose estimate is a bit off. Table 1 gives the posterior summaries for the estimated parameters of LCM-AR.

Table 1: Posterior summaries for LCM-AR simulated data

Parameter	True value	Posterior Mean	Posterior Std. Dev.
τ	300	455.422	109.925
β	0.200	0.206	0.003
$1/\sigma_1^2$	2.000	1.962	0.046
$1/\sigma_2^2$	2.000	1.909	0.037
$1/\sigma_3^2$	2.000	1.875	0.049
ρ_{12}	0.800	0.795	0.009
ρ_{13}	0.700	0.728	0.011
ρ_{23}	0.500	0.515	0.011
ϕ_{11}	0.800	0.730	0.010
ϕ_{22}	0.800	0.819	0.008
ϕ_{33}	0.800	0.807	0.007
$1/\sigma_{w1}^2$	3.333	3.312	0.044
$1/\sigma_{w2}^2$	5.000	5.438	0.059
$1/\sigma_{w3}^2$	2.000	2.149	0.021

Data from the trivariate LCM-VAR model with $Y_{j,it}$ ($i = 1, \dots, 30$; $j = 1, 2, 3$ and $t = 1, \dots, 500$) is simulated according to observation equation as in (17) and the state equation is described by

$$\mathbf{x}_t = \Phi \mathbf{x}_{t-1} + \mathbf{w}_t,$$

where

$$\Phi = \begin{pmatrix} 0.5 & 0 & 0.3 \\ 0.6 & 0.1 & 0.5 \\ 0.1 & 0 & 0.8 \end{pmatrix}$$

and \mathbf{w}_t is simulated from $N_3(\mathbf{0}, \mathbf{W})$, where $\mathbf{W} = \text{diag}(0.5, 0.25, 0.5)$, i.e., $W_1 = 0.5$, $W_2 = 0.25$ and $W_3 = 0.5$. The static predictor is simulated from $N(0, 1)$ and the coefficient $\beta = 0.2$. The level correlated term α_{it} is simulated from $N_3(\mathbf{0}, \Sigma)$, where Σ is defined as in (18) with $\sigma_1^2 = 1/3$, $\sigma_2^2 = 1/2$, $\sigma_3^2 = 1/3$ and $\rho_{12} = 0.6$, $\rho_{13} = 0.8$ and $\rho_{23} = 0.8$. The responses are simulated from gamma distribution with $\tau = 100$.

It took about 38 minutes to run LCM-VAR on the simulated data. Table 2 gives the posterior summaries for the estimated parameters of LCM-VAR. Similar to the LCM-AR simulation setup, most of the estimated parameters are close to their respective true values. The posterior standard deviation of the precisions of the state errors in LCM-VAR seems to be more than that in LCM-AR.

Table 2: Posterior summaries for LCM-VAR simulated data

Parameter	True value	Posterior Mean	Posterior Std. Dev.
τ	100	83.321	10.360
β	0.200	0.201	0.002
$1/\sigma_1^2$	3.000	3.109	0.038
$1/\sigma_2^2$	2.000	2.025	0.023
$1/\sigma_3^2$	3.000	3.115	0.038
ρ_{12}	0.600	0.644	0.007
ρ_{13}	0.800	0.847	0.006
ρ_{23}	0.800	0.843	0.005
ϕ_{11}	0.500	0.481	0.049
ϕ_{21}	0.600	0.569	0.030
ϕ_{31}	0.100	0.013	0.036
ϕ_{12}	0.000	-0.006	0.042
ϕ_{22}	0.100	0.090	0.031
ϕ_{32}	0.000	-0.041	0.039
ϕ_{13}	0.300	0.289	0.049
ϕ_{23}	0.500	0.517	0.025
ϕ_{33}	0.800	0.855	0.028
$1/\sigma_{w1}^2$	2.000	1.783	0.095
$1/\sigma_{w2}^2$	4.000	3.557	0.207
$1/\sigma_{w3}^2$	2.000	2.314	0.124

5 Modeling Multivariate Realized Volatility Measures

Volatility measurement is central to asset pricing, asset allocation, portfolio optimization and risk management. A first attempt to measure volatility using intraday data was made by Parkinson (1980) for the estimation of the daily range. Since then the literature has expanded significantly from the realized volatility of Andersen and Bollerslev (1998) to bipower variation (Barndorff-Nielsen and Shephard, 2004), realized kernels of Barndorff-Nielsen et al. (2009) and realized covariance matrices (Ait-Sahalia et al., 2010, Peluso et al., 2014). As these intraday volatility measures evolved, there has been a natural complementary effort to build adequate models to describe their joint dynamics (Engle and Gallo, 2006, Donelli et al., 2021, Cipollini et al., 2013).

5.1 Data description

The focus of this study is to model three robust intraday volatility measures: median realized variance (*MedRV*), realized kernel variance based on Parzen kernel (*RK*) and bipower variation (*BPV*) using the

different level correlated model specifications for the 30 stock indexes data (as shown in Table 3) available on Oxford-Man Institute’s Quantitative Finance Realized Library (Heber et al., 2009). These volatility measures are based on 5-minute sampling frequency. The sample period spans from January 2, 2015, to December 29, 2017. The number of observations for each stock index is 513. Thus we have $m = 3$, $n = 30$ and $T = 513$. In Table (3), we list all the stock indexes we have used in our analysis along with their associated regions.

Table 3: List of stock indexes along with their associated regions

Symbol	Name	Region
AEX	AEX index	Netherlands
AORD	All Ordinaries	Australia
BFX	Bell 20 Index	Belgium
BSESN	S&P BSE Sensex	India
BVSP	BVSP BOVESPA Index	United States
DJI	Dow Jones Industrial Average	United States
FCHI	CAC 40	France
FTMIB	FTSE MIB	Italy
FTSE	FTSE 100	United Kingdom
GDAXI	DAX	Germany
GSPTSE	S&P/TSX Composite index	Canada
HSI	HANG SENG Index	Hong Kong
IBEX	IBEX 35 Index	United States
IXIC	Nasdaq 100	United States
KS11	Korea Composite Stock Price Index	South Korea
KSE	Karachi SE 100 Index	Pakistan
MXX	IPC Mexico	Mexico
N225	Nikkei 225	Japan
NSEI	NIFTY 50	India
OMXC20	OMX Copenhagen 20 Index	Denmark
OMXHPI	OMX Helsinki All Share Index	Finland
OMXSPI	OMX Stockholm All Share Index	Sweden
OSEAX	Oslo Exchange All-share Index	Norway
RUT	Russel 2000	United States
SMSI	Madrid General Index	Spain
SPX	S&P 500 Index	United States
SSEC	Shanghai Composite Index	China
SSMI	Swiss Stock Market Index	Switzerland
STI	Straits Times Index	Singapore
STOXX50E	EURO STOXX 50	Europe

The mean, standard deviation (St.Dev.), skewness, kurtosis and autocorrelation of lag 1 of \sqrt{MedRV} , \sqrt{RK} and \sqrt{BPV} are given in Table (4). The values of skewness indicates that all of the realized measures are positively skewed and high values of kurtosis indicate the presence of heavy tails. All of the realized measures are persistent according to the high values of their first order autocorrelation.

Table 4: Descriptive Statistics of \sqrt{MedRV} , \sqrt{RK} and \sqrt{BPV}

	Mean	St.Dev.	Skewness	Kurtosis	AutoCorr(lag1)
\sqrt{MedRV}	0.004	0.003	2.314	13.094	0.750
\sqrt{RK}	0.007	0.005	3.487	30.008	0.583
\sqrt{BPV}	0.007	0.004	3.699	32.181	0.706

We compute the kendall’s correlation matrix for the components of the response vector in Table 5. The off-diagonal elements indicate high degree of positive correlation between the realized volatility measures.

Table 5: Kendall's correlation matrix of \sqrt{MedRV} , \sqrt{RK} and \sqrt{BPV}

	\sqrt{MedRV}	\sqrt{RK}	\sqrt{BPV}
\sqrt{MedRV}	1.00	0.62	0.77
\sqrt{RK}	0.62	1.00	0.72
\sqrt{BPV}	0.77	0.72	1.00

5.2 Realized Volatility Measures

Let $\{P_{t_j}\}$ be a sequence of observed intraday prices of an asset. Consider a time interval $[a, b]$ and the time index t_j for $t_j \in [a, b]$. The time is partitioned into M equidistant points in time $j = 1, \dots, M$. At each time point t_j , the price of an asset is observed. Then $\{P_{t_j}\}_{j=1}^M$ is the observed sequence of prices of an asset sampled at frequency $\tau = \frac{b-a}{M-1}$. Hence the intraday returns over the sub-interval $[t_{j-1}, t_j]$ is defined as $r_j = \log(P_{t_j}) - \log(P_{t_{j-1}})$. To obtain realized variances at 5-minutes sampling frequency, $\tau = 300$ seconds and similarly for 1-minute sampling frequency, $\tau = 60$ seconds.

Let us denote $r_{j,t}$ as the j^{th} intraday return for t^{th} day, for $t = 1, \dots, T$. We define some popular measures of intraday volatility considered in the literature. Median realized variance ($MedRV$) is an estimator introduced by Andersen et al. (2012), which is a scaled square of the median of three consecutive intraday absolute returns, which is calculated as

$$MedRV_t = \frac{\pi}{6 - 4\sqrt{3} + \pi} \frac{M}{M-2} \sum_{j=2}^{M-1} \text{median}(|r_{j-1,t}|, |r_{j,t}|, |r_{j+1,t}|)^2.$$

Barndorff-Nielsen et al. (2009) proposed the realized kernels estimator, which uses kernel methods to combat market microstructure noise. The realized kernel estimator is

$$RK_t = \sum_{h=-H}^H k\left(\frac{h}{H+1}\right) \gamma_h, \quad \text{where}$$

$$\gamma_h = \sum_{i=|h|+1}^n r_{i,t} r_{i-|h|,t},$$

where $k(\cdot)$ is the Parzen kernel function defined as

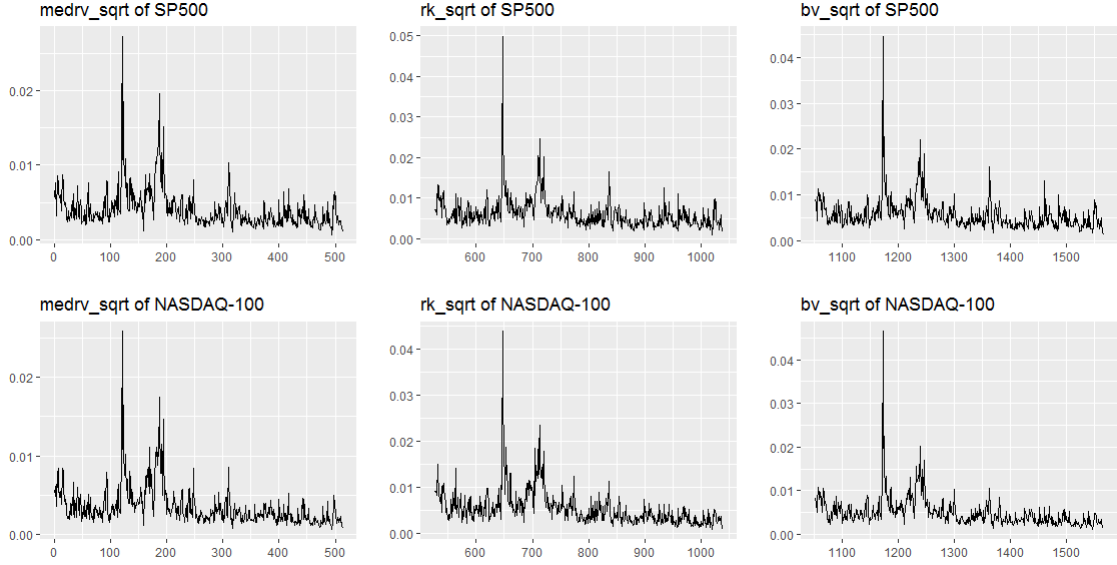
$$k(x) = \begin{cases} 1 - 6x^2 + 6x^3 & 0 \leq x \leq 1/2 \\ 2(1-x)^3 & 1/2 \leq x \leq 1 \\ 0 & x > 1. \end{cases}$$

A simple and comprehensible measure, which isolates the variation of the pure price process is the Bipower variation (BPV). It is calculated as the sum of products of absolute values of two consecutive returns,

$$BPV_t = \sum_{j=2}^M |r_{j,t}| |r_{j-1,t}|.$$

For each day t , we consider the $m = 3$ -dimensional time series composed of standard deviation versions of median realized variance, realized kernel and bipower variation, $\mathbf{y}_t = (\sqrt{MedRV}_t, \sqrt{RK}_t, \sqrt{BPV}_t)'$, where $t = 1, \dots, T$. We have plotted the time series of \sqrt{MedRV} , \sqrt{RK} and \sqrt{BPV} for two stock indexes S&P 500 and NASDAQ-100 for illustration.

Figure 1: Plots of \sqrt{MedRV} , \sqrt{RK} and \sqrt{BPV} for SP500 and NASDAQ-100 from January 2, 2015, to December 29, 2017



5.3 Model Specification

Let $\mathbf{y}_{it} = (y_{1,it}, \dots, y_{m,it})'$ be a m -variate vector of positive-valued volatility measures over time, for $i = 1, \dots, n$ and $t = 1, \dots, T$. That is, we observe m components of different volatility measures on n stock market indexes over T regularly spaced time points. High values of the lag 1 autocorrelation has prompted us to use $\log(Y_{j,i,t-1})$ as the predictor indicating the daily level component driven by short term traders as in Corsi (2009). We define the daily jump component as $J_t = \max(RV_t - BPV_t, 0)$ and the daily continuous component as $C_t = RV_t - J_t$, where $RV_t = \sum_{j=1}^M r_{j,t}^2$, is the realized variance at time t . The daily jump and continuous components account for the jumps in the price process, and are useful predictors in modeling realized volatility (Andersen et al., 2007). With these predictors, (1) – (2) simplify as

$$Y_{j,it} | \theta_{j,it}, \tau \sim \text{Gamma}\left(\tau, \frac{\tau}{\theta_{j,it}}\right), \quad (19)$$

$$\log(\theta_{j,it}) = \alpha_{j,i} + \beta_{j,t,0} + \beta_{1,j} \log(Y_{j,i,t-1}) + \beta_{2,j} \log(1 + J_{j,i,t-1}) + \beta_{3,j} \log(1 + C_{j,i,t-1}) + \xi_{j,it},$$

where the level $\alpha_{j,i}$ is assumed to be stock-specific, and the level correlated effect $\boldsymbol{\xi} = (\xi_{1,it}, \xi_{2,it}, \xi_{3,it})' \sim N(\mathbf{0}, \boldsymbol{\Sigma})$, with

$$\boldsymbol{\Sigma} = \begin{pmatrix} \sigma_1^2 & \rho_{12}\sigma_1\sigma_2 & \rho_{13}\sigma_1\sigma_3 \\ \rho_{12}\sigma_1\sigma_2 & \sigma_2^2 & \rho_{23}\sigma_2\sigma_3 \\ \rho_{13}\sigma_1\sigma_3 & \rho_{23}\sigma_2\sigma_3 & \sigma_3^2 \end{pmatrix}.$$

We refer to this model as LCM1, and consider two different specifications for the time-varying intercept $\beta_{j,t,0}$, similar to (3) and (5). First, an assumption of VAR evolution leads to

$$\beta_{t,0} = \boldsymbol{\Phi}\beta_{t-1,0} + \mathbf{w}_t, \text{ where } \mathbf{w}_t \sim N(\mathbf{0}, \mathbf{W}), \quad (20)$$

while an AR specification for each component $j = 1, \dots, m$ leads to

$$\beta_{j,t,0} = \phi_j \beta_{j,t-1,0} + w_{j,t}, \text{ where } w_{j,t} \sim N(0, W_j). \quad (21)$$

We refer to (19) and (20) as LCM1-VAR, and to (19) and (21) as LCM1-AR.

We also investigate a setup where the level $\alpha_{j,i}$ is component-specific but *not* stock-specific, and define the corresponding model LCM2 as

$$Y_{j,it}|\theta_{j,it} \sim \text{Gamma}\left(\tau, \frac{\tau}{\theta_{j,it}}\right), \quad (22)$$

$$\log(\theta_{j,it}) = \alpha_j + \beta_{j,t,0} + \beta_{1,j} \log(Y_{j,i,t-1}) + \beta_{2,j} \log(1 + J_{j,i,t-1}) + \beta_{3,j} \log(1 + C_{j,i,t-1}) + \xi_{j,it},$$

In this case, we refer to equations (22) and (20) as LCM2-VAR, and to (22) and (21) as LCM2-AR. The difference between LCM1 and LCM2 lies in the specification of the level α .

5.4 Results

Using **R-INLA**, we fit the four models discussed in Section (5.3): LCM1-VAR, LCM1-AR, LCM2-VAR, and LCM2-AR, using the same prior specification as mentioned in Section (3.2). We have assumed $\tau \sim \text{Gamma}(1, 0.1)$ such that $E[\tau] = 10$ and $\text{Var}[\tau] = 100$.

In Table 6, we show the mean of the posterior means of the levels from Model LCM1. We also show the posterior mean of the levels from Model LCM2.

Table 6: Posterior summaries of component-specific levels

	LCM1-VAR	LCM1-AR	LCM2-VAR	LCM2-AR
Parameter	Mean of Posterior Mean	Mean of Posterior Mean	Posterior Mean	Posterior Mean
α_1	-4.401	-4.898	-3.312	-3.869
α_2	-4.443	-4.633	-3.657	-3.923
α_3	-3.864	-4.450	-3.062	-3.583

In Table 7, we show posterior summaries of the covariate coefficients and hyperparameters for Models LCM1 and LCM2. We observe that the β 's corresponding to the daily effects are higher under the AR specification than those obtained by assuming a VAR(1) state evolution, whereas the estimated state precisions are higher for the VAR(1) state evolution than the AR(1) state evolution. The estimated level correlations among the three volatility measures, i.e., ρ_{12} , ρ_{13} and ρ_{23} , across all the models are strong and significant, which empirically confirms dependency between them. The estimated level correlations from the four models are close to the Kendall's tau as discussed in Table (5). Most of the estimated parameters are significant except for the jump components.

Table 7: Posterior summaries of covariate coefficients and hyperparameters

	LCM1-VAR	LCM1-AR	LCM2-VAR	LCM2-AR
Parameter	Posterior Mean	Posterior Mean	Posterior Mean	Posterior Mean
Covariate coefficients				
$\beta_{1,1}$	0.206	0.120	0.405	0.306
$\beta_{1,2}$	0.122	0.088	0.281	0.229
$\beta_{1,3}$	0.244	0.133	0.404	0.303
$\beta_{2,1}$	1.661	42.829	5.444	36.690
$\beta_{2,2}$	14.860	31.900	-23.530	8.912
$\beta_{2,3}$	21.604	57.976	6.873	37.788
$\beta_{3,1}$	263.115	307.014	220.804	295.162
$\beta_{3,2}$	227.402	273.007	249.234	291.896
$\beta_{3,3}$	183.556	245.000	186.188	268.420
Hyperparameters				
$1/\sigma_1^2$	13.034	11.177	11.472	9.030
$1/\sigma_2^2$	9.128	7.431	7.672	6.649
$1/\sigma_3^2$	17.758	13.290	15.152	11.019
ρ_{12}	0.621	0.677	0.605	0.676
ρ_{13}	0.811	0.854	0.802	0.859
ρ_{23}	0.807	0.837	0.798	0.841
ϕ_{11}	2.419	0.996	0.134	0.997
ϕ_{21}	2.564		0.309	
ϕ_{31}	2.464		0.444	
ϕ_{12}	0.592		2.482	
ϕ_{22}	0.623	0.996	2.496	0.998
ϕ_{32}	0.526		2.362	
ϕ_{13}	-2.318		-2.205	
ϕ_{23}	-2.382		-2.246	
ϕ_{33}	-2.359	0.997	-2.410	0.998
$1/W_1$	428.255	20.633	768.665	32.634
$1/W_2$	173.920	21.040	458.162	29.387
$1/W_3$	667.143	25.496	868.763	41.081

5.5 Model Comparisons

In volatility modeling, we are mostly interested in out-of-sample forecasting accuracy. We compare the four models discussed in section 5.4 using popular measures such as mean absolute percentage error (MAPE) and mean absolute error (MAE). Let $y_{n_t}(l)$ be the l^{th} step-ahead forecast from origin n_t for y_{t+l} , $l = 1, \dots, n_h$, and let $e_{n_t}(l) = y_{n_t+l} - y_{n_t}(l)$ be the l^{th} step-ahead forecast error. MAPE is defined as

$$\text{MAPE} = \frac{1}{n_h} \sum_{l=1}^{n_h} |e_{n_t}(l)/y_{n_t+l}|.$$

MAE is defined as

$$\text{MAE} = \frac{1}{n_h} \sum_{l=1}^{n_h} |e_{n_t}(l)|.$$

Small values of MAPE and MAE indicate better model. To evaluate forecast accuracy, for each stock index and each realized volatility measure we calculated both MAPE and MAE based on 1-step, 5-step and 10-step ahead forecasts i.e. for $n_h = 1, 5$ and 10. In Table (8), we compute MAPE and MAE as the average across stock indexes and across the realized volatility measures.

Table 8: MAPE and MAE averaged across the 30 stock indexes and also across 3 realized volatility measures

Horizon (n_h)	LCM1-AR	LCM1-VAR	LCM2-AR	LCM2-VAR
MAPE				
1	0.302	0.320	0.310	0.282
5	0.307	0.322	0.318	0.252
10	0.317	0.367	0.324	0.280
MAE				
1	0.0012	0.0013	0.0013	0.0011
5	0.0012	0.0014	0.0012	0.0010
10	0.0013	0.0016	0.0012	0.0011

Thus, based on MAPE and MAE, LCM2-VAR outperforms all other models. For in-sample comparison we have used Deviance Information Criterion (DIC) (Spiegelhalter et al., 2002) as the model selection criterion. In that case, LCM1-AR was outperforming the rest due to smaller values of DIC, but this model does not perform well in terms of forecasting accuracy as in Table 8.

6 Summary and discussion

This article describes the use of the `rgeneric()` function in R-INLA for fitting an LCM with VAR(p) latent effects to vector positive-valued time series. We demonstrate the method using simulated data and realized financial volatilities. The proposed LCM-VAR framework is not limited to financial applications, or to temporal models with exogenous predictors. We can easily adapt the model to incorporate spatial dependence between different locations, with applications in modeling climate variables.

Another useful direction is a hierarchical multivariate dynamic model (HMMDM) setup where the observed data vector $\mathbf{y}_{it} = (Y_{1,it}, \dots, Y_{m,it})'$ follows a multivariate Gamma distribution. Several multivariate extensions of the univariate gamma distributions exist in the literature (see Cherian (1941), Ramabhadran (1951), Mathai and Moschopoulos (1991), and Kotz et al. (2004) and references therein). Here we define multivariate gamma distribution as defined in (Tsonas, 2004) which is in the same spirit as in (Mathai and Moschopoulos, 1991). Following (Mathai and Moschopoulos, 1991) and (Tsonas, 2004) to define the probability distribution function (p.d.f.) of an m -variate gamma distribution, we assume that

$$Y_{j,it} = V_{j,it} + Z,$$

where $V_{j,it}$ and Z are independent random variables distributed as Gamma($\lambda_{j,it}, \theta_{j,it}$), $i = 1, \dots, n$, $j = 1, \dots, m$, $t = 1, \dots, T$ and Gamma(α, γ) respectively. Then for $i = 1, \dots, n$, $j = 1, \dots, m$ and $t = 1, \dots, T$,

$$p(y_{j,it}|z, \lambda_{j,it}, \theta_{j,it}) = \frac{\theta_{j,it}^{\lambda_{j,it}}}{\Gamma(\lambda_{j,it})} (y_{j,it} - z)^{\lambda_{j,it}-1} \exp[-\theta_{j,it}(y_{j,it} - z)], \quad y_{j,it} \geq z,$$

and the p.d.f. of z is given by

$$p(z|\alpha, \gamma) = \frac{\gamma^\alpha}{\Gamma(\alpha)} z^{\alpha-1} \exp(-\gamma z), \quad z > 0, \alpha > 0, \gamma > 0.$$

The sampling distribution is given by

$$p(\mathbf{y}_{it}|\alpha, \gamma, \boldsymbol{\lambda}_{it}, \boldsymbol{\theta}_{it}) = \frac{\gamma^\alpha}{\Gamma(\alpha)} \prod_{j=1}^m \frac{\theta_{j,it}^{\lambda_{j,it}}}{\Gamma(\lambda_{j,it})} \int_0^B (y_{j,it} - z)^{\lambda_{j,it}-1} \exp(-\theta_{j,it}(y_{j,it} - z)) z^{\alpha-1} \exp(-\gamma z) dz,$$

where $B = \min\{y_{j,it} : i = 1, \dots, n; j = 1, \dots, m; t = 1, \dots, T\}$, $\boldsymbol{\lambda}_{it} = (\lambda_{1,it}, \dots, \lambda_{m,it})'$, $\boldsymbol{\theta}_{it} = (\theta_{1,it}, \dots, \theta_{m,it})'$ and $\boldsymbol{\Theta}_{it} = (\boldsymbol{\lambda}_{it}, \boldsymbol{\theta}_{it})'$ and $\alpha > 0, \gamma > 0$. The second-level observational equation for $i = 1, \dots, n$, $j = 1, \dots, m$ and $t = 1, \dots, T$ is given by

$$\log(\boldsymbol{\Theta}_{j,it}) = \mathbf{D}'_{j,it} \boldsymbol{\delta}_{j,it} + \mathbf{S}'_{j,it} \boldsymbol{\eta}_{j,it},$$

where $\mathbf{D}_{j,it} = (D_{j,it,1}, \dots, D_{j,it,a_j})'$ is an a_j -dimensional vector of exogenous predictors with stock-time varying (dynamic) coefficients $\boldsymbol{\delta}_{j,it} = (\delta_{j,it,1}, \dots, \delta_{j,it,a_j})'$ and $\mathbf{S}_{j,it} = (S_{j,it,1}, \dots, S_{j,it,b_j})'$ is a b_j -dimensional vector of exogenous predictors with static coefficients $\boldsymbol{\eta}_j = (\eta_{j,1}, \dots, \eta_{j,it,b_j})'$. Let $\boldsymbol{\xi}_{it}$ be a p_d -dimensional vector constructed by stacking the a_j coefficients $\boldsymbol{\delta}_{j,it}$ for $j = 1, \dots, m$. The structural equation of the HMDM relates the stock-time varying parameter $\boldsymbol{\xi}_{it}$ to an aggregate (pooled) state parameter \mathbf{x}_t :

$$\boldsymbol{\xi}_{it} = \mathbf{x}_t + \mathbf{v}_{it}$$

where the errors \mathbf{v}_{it} are assumed to be i.i.d. $N_{p_d}(\mathbf{0}, \mathbf{V}_i)$. The state (or system) equation of the HMDM is:

$$\mathbf{x}_t = \mathbf{G}\mathbf{x}_{t-1} + \mathbf{w}_t$$

where \mathbf{G} is a $p_d \times p_d$ state transition matrix and the state errors \mathbf{w}_t are assumed to be i.i.d. $N_{p_d}(\mathbf{0}, \mathbf{W})$. This model could be explored in the context of analyzing the joint dynamics of stock indexes. Although we have not discussed about incorporating dependence between the components of \mathbf{Y} through copulas, this could be an interesting topic for further exploration.

Appendix

rgeneric() construction for VAR(1)

In this section we briefly explain how to build an `rmodel` to fit latent VAR(1) using `rgeneric()` in R-INLA. We have to define `rmodel` that we label '`inla.rgeneric.VAR1.model`'. Through the `inla.rgeneric.define()` function, we create an `inla.rgeneric` object that we call `model.VAR`.

```
model.VAR <- inla.rgeneric.define(inla.rgeneric.VAR1.model, ...)
```

Then, we can embed this "inla.rgeneric" object in the usual INLA syntax to fit latent VAR(1).

```
formula.inla <- ... + f(idx, model = model.VAR, ...) + ...,
```

where `idx` refers to the indices in R-INLA setup.

Let \mathbf{x}_t be a m -dimensional time series following VAR(1) process as in equation (7). Assuming $\mathbf{W} = \text{diag}(\sigma_{w1}^2, \dots, \sigma_{wm}^2)$, be the $m \times m$ covariance matrix of the latent states. The set of parameters in latent VAR(1) consists of $\{\phi_{ij}, i = 1, \dots, m; j = 1, \dots, m\}$ and the marginal variances σ_{wj}^2 , for $j = 1, \dots, m$. For the internal representation of the parameters in INLA, we transform the marginal variances into log-precisions such that $\boldsymbol{\theta} = (\phi_{11}, \phi_{21}, \dots, \phi_{mm}, \log(1/\sigma_{w1}^2), \dots, \log(1/\sigma_{wm}^2))'$ such that each of its components has \mathbb{R} as its support, as required by R-INLA. For more details about how to build an `rgeneric()` function, `vignette("rgeneric", package= "INLA")` line in R provides documentation.

In order to define latent VAR(1), we need to construct '`inla.rgeneric.VAR1.model`', which returns several functions such as `Q()`, `graph()`, `mu()`, `log.prior()`, `initial()`, `log.norm.const()`, etc.

- The `Q()` function defines the precision matrix of the VAR(1) process which is derived in (8).
- The `graph()` function defines the 0/1 representation of the precision matrix indicating the zero and non-zero entries of the precision matrix as returned by `Q()`.
- The `mu()` function returns $\mathbf{0}$.
- We assign a Gaussian prior $\mathcal{N}(\text{mean} = \mu, \text{variance} = \sigma^2)$ on ϕ_{ij} , for $i = 1, \dots, m, j = 1, \dots, m$ and Gamma prior $\Gamma(\cdot, a; b)$ (with mean a/b and variance a/b^2) on the precisions, $1/\sigma_{wj}^2, j = 1, \dots, m$. Hence the joint prior for $\boldsymbol{\theta}$ becomes

$$\pi(\boldsymbol{\theta}) = \prod_{i=1}^{m^2} \mathcal{N}(\theta_i, 1; 1) \times \prod_{j=m^2+1}^{m^2+m} \Gamma(\theta_j; 1, 1) \times \exp(\theta_j), \quad (23)$$

where for each $j = m^2 + 1, \dots, m^2 + m$, $\exp(\theta_j)$ is the Jacobian for the change of variable from $1/\sigma_j^2$ to $\theta_j = \log(1/\sigma_{wj}^2)$. Hence the `log.prior()` returns the logarithm of the joint prior as in (23).

- We have defined the initial values of $\phi_{ij} = 0.1$ and precisions $1/\sigma_{wj}^2$ as 1 for $i = 1, \dots, m$ and $j = 1, \dots, m$. The function `initial()` contains the initial values of the parameter $\boldsymbol{\theta}$ in the internal scale.
- The `log.norm.const()` denotes the logarithm of the normalizing constant from a multivariate Gaussian distribution.

References

- Y. Aït-Sahalia, J. Fan, and D. Xiu. High-frequency covariance estimates with noisy and asynchronous financial data. *Journal of the American Statistical Association*, 105(492):1504–1517, 2010.
- J. Aitchison and C. Ho. The multivariate poisson-log normal distribution. *Biometrika*, 76(4):643–653, 1989.
- T. Aktekin, N. G. Polson, and R. Soyer. A family of multivariate non-gaussian time series models. *Journal of Time Series Analysis*, 41(5):691–721, 2020.
- T. G. Andersen and T. Bollerslev. Answering the skeptics: Yes, standard volatility models do provide accurate forecasts. *International Economic Review*, pages 885–905, 1998.
- T. G. Andersen, T. Bollerslev, and F. X. Diebold. Roughing it up: Including jump components in the measurement, modeling, and forecasting of return volatility. *The Review of Economics and Statistics*, 89(4):701–720, 2007.
- T. G. Andersen, D. Dobrev, and E. Schaumburg. Jump-robust volatility estimation using nearest neighbor truncation. *Journal of Econometrics*, 169(1):75–93, 2012.
- O. E. Barndorff-Nielsen and N. Shephard. Power and bipower variation with stochastic volatility and jumps. *Journal of Financial Econometrics*, 2(1):1–37, 2004.
- O. E. Barndorff-Nielsen, P. R. Hansen, A. Lunde, and N. Shephard. Realized kernels in practice: Trades and quotes. *The Econometrics Journal*, 2009.
- M. A. Benjamin, R. A. Rigby, and D. M. Stasinopoulos. Generalized autoregressive moving average models. *Journal of the American Statistical Association*, 98(461):214–223, 2003.
- K. Cherian. A bi-variate correlated gamma-type distribution function. *The Journal of the Indian Mathematical Society*, 5:133–144, 1941.
- S. Chib and R. Winkelmann. Markov chain monte carlo analysis of correlated count data. *Journal of Business & Economic Statistics*, 19(4):428–435, 2001.
- Chiogna, M. Carlo Gaetan, and C. Gaetan. Dynamic generalized linear models with application to environmental epidemiology. *Journal of the Royal Statistical Society: Series C (Applied Statistics)*, 51(4):453–468, 2002.
- F. Cipollini, R. F. Engle III, and G. M. Gallo. Vector multiplicative error models: representation and inference. *Working Paper Series, NBER*, 2006.
- F. Cipollini, R. F. Engle, and G. M. Gallo. Semiparametric vector MEM. *Journal of Applied Econometrics*, 28(7):1067–1086, 2013.
- F. Corsi. A simple approximate long-memory model of realized volatility. *Journal of Financial Econometrics*, 7(2):174–196, 2009.
- N. Donelli, S. Peluso, and A. Mira. A Bayesian semiparametric vector multiplicative error model. *Computational Statistics & Data Analysis*, 161:107242, 2021.
- J. Durbin and S. J. Koopman. *Time Series Analysis by State Space Methods*, volume 38. OUP Oxford, 2012.
- R. F. Engle and G. M. Gallo. A multiple indicators model for volatility using intra-daily data. *Journal of Econometrics*, 131(1-2):3–27, 2006.
- L. Fahrmeir and H. Kaufmann. Regression models for non-stationary categorical time series. *Journal of Time Series Analysis*, 8(2):147–160, 1987.
- L. Fahrmeir, G. Tutz, W. Hennevogl, and E. Salem. *Multivariate Statistical Modelling Based on Generalized Linear Models*, volume 425. Springer, 1994.

- J. L. Gallego. The exact likelihood function of a vector autoregressive moving average process. *Statistics & Probability Letters*, 79(6):711–714, 2009.
- D. Gamerman. Markov chain monte carlo for dynamic generalised linear models. *Biometrika*, 85(1):215–227, 1998.
- D. P. Gaver and P. Lewis. First-order autoregressive gamma sequences and point processes. *Advances in Applied Probability*, 12(3):727–745, 1980.
- E. Godolphin and K. Triantafyllopoulos. Decomposition of time series models in state-space form. *Computational Statistics & Data Analysis*, 50(9):2232–2246, 2006.
- C. Gouriéroux and J. Jasiak. Autoregressive gamma processes. *Journal of Forecasting*, 25(2):129–152, 2006.
- G. K. Grunwald, P. Guttorp, and A. E. Raftery. Prediction rules for exponential family state space models. *Journal of the Royal Statistical Society: Series B (Methodological)*, 55(4):937–943, 1993.
- N. Hautsch, O. Okhrin, and A. Ristig. Modeling time-varying dependencies between positive-valued high-frequency time series. In *Copulae in Mathematical and Quantitative Finance*, pages 115–127. Springer, 2013.
- G. Heber, A. Lunde, N. Shephard, and K. Sheppard. Oxford-Man Institute’s realized library, version 0.1, 2009.
- P. Jacobs and P. Lewis. A mixed autoregressive-moving average exponential sequence and point process (EARMA (1, 1)). *Advances in Applied Probability*, 9(1):87–104, 1977.
- S. Kotz, N. Balakrishnan, and N. L. Johnson. *Continuous Multivariate Distributions, Volume 1: Models and Applications*, volume 1. John Wiley & Sons, 2004.
- A. Lawrance and P. Lewis. The exponential autoregressive-moving average earma (p, q) process. *Journal of the Royal Statistical Society: Series B (Methodological)*, 42(2):150–161, 1980.
- A. Lawrance and P. Lewis. A new autoregressive time series model in exponential variables (near (1)). *Advances in Applied Probability*, 13(4):826–845, 1981.
- A. Lawrance and P. Lewis. Modelling and residual analysis of nonlinear autoregressive time series in exponential variables. *Journal of the Royal Statistical Society: Series B (Methodological)*, 47(2):165–183, 1985.
- F. Lindgren and H. Rue. Bayesian spatial modelling with R-INLA. *Journal of statistical software*, 63:1–25, 2015.
- J. K. Lindsey and P. Lambert. Dynamic generalized linear models and repeated measurements. *Journal of Statistical Planning and Inference*, 47(1-2):129–139, 1995.
- H. Lütkepohl. *New Introduction to Multiple Time Series Analysis*. Springer Science & Business Media, 2005.
- J. Ma, K. M. Kockelman, and P. Damien. A multivariate poisson-lognormal regression model for prediction of crash counts by severity, using Bayesian methods. *Accident Analysis & Prevention*, 40(3):964–975, 2008.
- T. G. Martins, D. Simpson, F. Lindgren, and H. Rue. Bayesian computing with INLA: new features. *Computational Statistics & Data Analysis*, 67:68–83, 2013.
- A. M. Mathai and P. G. Moschopoulos. On a multivariate gamma. *Journal of Multivariate Analysis*, 39(1):135–153, 1991.
- F. Palmí-Perales, V. Gómez-Rubio, and M. A. Martínez-Beneito. Bayesian multivariate spatial models for lattice data with inla. *Journal of Statistical Software*, 98(2):1–29, 2021. doi: 10.18637/jss.v098.i02. URL <https://www.jstatsoft.org/index.php/jss/article/view/v098i02>.

- M. Parkinson. The extreme value method for estimating the variance of the rate of return. *Journal of Business*, pages 61–65, 1980.
- S. Peluso, F. Corsi, and A. Mira. A Bayesian high-frequency estimator of the multivariate covariance of noisy and asynchronous returns. *Journal of Financial Econometrics*, 13(3):665–697, 2014.
- G. Petris. An R package for Dynamic Linear Models. *Journal of Statistical Software*, 36:1–16, 2010.
- A. Prékopa and T. Szántai. A new multivariate gamma distribution and its fitting to empirical streamflow data. *Water Resources Research*, 14(1):19–24, 1978.
- A. Raftery. Generalized non-normal time series models. *Time series analysis: Theory and practice*, 1(0): 621–640, 1982.
- V. Ramabhadran. A multivariate gamma-type distribution. *Sankhyā: The Indian Journal of Statistics*, pages 45–46, 1951.
- H. Rue and L. Held. *Gaussian Markov Random Fields: Theory and Applications*. Chapman and Hall/CRC, 2005.
- H. Rue, S. Martino, and N. Chopin. Approximate Bayesian inference for latent Gaussian models by using integrated nested Laplace approximations. *Journal of the Royal Statistical Society: Series B (Statistical Methodology)*, 71(2):319–392, 2009.
- R. Ruiz-Cárdenas, E. T. Krainski, and H. Rue. Direct fitting of dynamic models using integrated nested laplace approximations—INLA. *Computational Statistics & Data Analysis*, 56(6):1808–1828, 2012.
- V. Serhiyenko. Dynamic modeling of multivariate counts-fitting, diagnostics, and applications. *PhD Thesis, University of Connecticut*, 2015.
- V. Serhiyenko, N. Ravishanker, and R. Venkatesan. Approximate Bayesian estimation for multivariate count time series models. In *Ordered Data Analysis, Modeling and Health Research Methods*, pages 155–167. Springer, 2015.
- V. Serhiyenko, N. Ravishanker, and R. Venkatesan. Multi-stage multivariate modeling of temporal patterns in prescription counts for competing drugs in a therapeutic category. *Applied Stochastic Models in Business and Industry*, 34(1):61–78, 2018.
- N. Shephard and M. K. Pitt. Likelihood analysis of non-gaussian measurement time series. *Biometrika*, 84(3):653–667, 1997.
- D. J. Spiegelhalter, N. G. Best, B. P. Carlin, and A. Van Der Linde. Bayesian measures of model complexity and fit. *Journal of the Royal Statistical Society: Series B (Statistical Methodology)*, 64(4):583–639, 2002.
- E. G. Tsonas. Bayesian inference for multivariate gamma distributions. *Statistics and Computing*, 14(3): 223–233, 2004.
- M. West and J. Harrison. *Bayesian Forecasting and Dynamic Models*. Springer Science & Business Media, 2006.
- M. West, P. J. Harrison, and H. S. Migon. Dynamic generalized linear models and bayesian forecasting. *Journal of the American Statistical Association*, 80(389):73–83, 1985.
- S. Yue. A bivariate gamma distribution for use in multivariate flood frequency analysis. *Hydrological Processes*, 15(6):1033–1045, 2001.